The Astrophysical Journal, 679:1422–1426, 2008 June 1

SPIN DIAGRAMS FOR EQUAL-MASS BLACK HOLE BINARIES WITH ALIGNED SPINS

Luciano Rezzolla,[1,2] Ernst Nils Dorband,[1] Christian Reisswig,[1] Peter Diener,[2,3]
Denis Pollney,[1] Erik Schnetter,[2,3] and Béla Szilágyi[1]
Received 2007 August 29; accepted 2008 February 19

ABSTRACT

Binary black hole systems with spins aligned with the orbital angular momentum are of special interest, as they may be the preferred end state of the inspiral of generic supermassive binary black hole systems. In view of this, we have computed the inspiral and merger of a large set of binary systems of equal-mass black holes with spins aligned with the orbital angular momentum but otherwise arbitrary. By least-square fitting the results of these simulations, we have constructed two "spin diagrams" which provide straightforward information about the recoil velocity $|v_{\rm kick}|$ and the final black hole spin $a_{\rm fin}$ in terms of the dimensionless spins a_1 and a_2 of the two initial black holes. Overall, they suggest a maximum recoil velocity of $|v_{\rm kick}| \simeq 441.94$ km s^{-1}, and minimum and maximum final spins $a_{\rm fin} \simeq 0.3471$ and $a_{\rm fin} = 0.9591$, respectively.

Subject headings: black hole physics — gravitational waves — relativity — stars: statistics

Online material: color figures

1. INTRODUCTION

A number of recent developments in numerical relativity have allowed for stable evolution of binary black holes and opened the door to extended and systematic studies of these systems. Of particular interest to astrophysics are the calculations of the recoil velocity and of the spin of the final black hole produced by the merger. It is well known that a binary with unequal masses or spins will radiate gravitational energy asymmetrically. This results in an uneven flux of momentum, providing a net linear velocity to the final black hole. The knowledge of both the "kick" velocity and the final spin could have a direct impact on studies of the evolution of supermassive black holes and on statistical studies on the dynamics of compact objects in dense stellar systems.

Over the past year, a number of simulations have been carried out to determine the recoil velocities for a variety of binary black hole systems. Nonspinning but unequal-mass binaries were the first systems to be studied, and several works have now provided an accurate mapping of the unequal-mass space of parameters (Herrmann et al. 2007a; Baker et al. 2006b; Gonzalez et al. 2007b). More recently, the recoils from binaries with spinning black holes have also been considered by investigating equal-mass binaries in which the spins of the black holes are either aligned with the orbital angular momentum (Herrmann et al. 2007b; Koppitz et al. 2007), or not. In the first case, a systematic investigation has shown that the largest recoil possible from such systems is of the order of 450 km s^{-1} (Pollney et al. 2007). In the second case, instead, specific configurations with spins orthogonal to the orbital one have been shown to lead to recoils as high as 2500 km s^{-1} (Campanelli et al. 2007a; Gonzalez et al. 2007a), suggesting a maximum kick of about 4000 km s^{-1} for maximally spinning black holes (Campanelli et al. 2007b). Recoil velocities of this magnitude could lead to the ejection of massive black holes from the hosting galaxies, with important consequences for their cosmological evolution.

Here, we extend the analysis carried out in Pollney et al. (2007) of binary black hole systems with equal mass and spins aligned with the orbital one. Our interest in this type of binary stems from the fact that systems of this type may represent a preferred end state of binary evolution. Post-Newtonian studies have shown that in vacuum the gravitational spin-orbit coupling has a tendency to align the spins when they are initially close to the orbital one (Schnittman 2004). Furthermore, if the binary evolves in a disk, as expected for supermassive black holes, the matter can exert a torque tending to align the spins (Bogdanovic et al. 2007). Finally, a recoiling supermassive black hole could retain the inner part of its accretion disk and thus the fuel for a continuing QSO phase lasting millions of years as it moves away from the galactic nucleus (Loeb 2007). Yet, the analysis of QSOs from the Sloan Digital Sky Survey shows no evidence for black holes carrying an accretion disk and hence for very large recoiling velocities (Bonning et al. 2007).

2. NUMERICAL SETUP AND INITIAL DATA

The numerical simulations have been carried out using the CCATIE code, a three-dimensional finite-differences code using the Cactus Computational Toolkit[4] and the Carpet mesh-refinement infrastructure (Schnetter et al. 2004). The main features of the code have been recently reviewed in Pollney et al. (2007), where the code has been employed using the so-called "moving-punctures" technique (Baker et al. 2006a; Campanelli et al. 2006a). The initial data consists of five sequences with constant orbital angular momentum, which is however different from sequence to sequence. In the *r* and *ra*-sequences, the initial spin of one of the black holes, $\mathbf{S}_2$, is held fixed along the *z*-axis, and the spin of the other black hole is varied so that the spin ratio a_1/a_2 takes the values between -1 and $+1$, with $a_i \equiv \mathbf{S}_i/M_i^2$. In the *t*-sequence, instead, the spin with a negative *z*-component is held fixed, while in the *s* and *u*-sequences $a_1/a_2 = 1$ and -1, respectively. In all cases, the masses are $M_i = M/2 = 1/2$. For the orbital initial data parameters, we use the effective-potential

[1] Max-Planck-Institut für Gravitationsphysik, Albert-Einstein-Institut, Potsdam-Golm, Germany.
[2] Department of Physics and Astronomy, Louisiana State University, Baton Rouge, LA.
[3] Center for Computation and Technology, Louisiana State University, Baton Rouge, LA.

[4] Available at: http://www.cactuscode.org.

TABLE 1

BINARY SEQUENCES FOR WHICH NUMERICAL SIMULATIONS HAVE BEEN CARRIED OUT

Sequence (1)	$\pm x/M$ (2)	$\pm p/M$ (3)	m_1/M (4)	m_2/M (5)	a_1 (6)	a_2 (7)	$\tilde{M}_{\rm ADM}$ (8)	$\tilde{J}_{\rm ADM}$ (9)	$\lvert v_{\rm kick}\rvert$ (10)	$\lvert v^{\rm fit}_{\rm kick}\rvert$ (11)	Error (%) (12)	$a_{\rm fin}$ (13)	$a^{\rm fit}_{\rm fin}$ (14)	Error (%) (15)
*r*0	3.0205	0.1366	0.4011	0.4009	−0.584	0.584	0.9856	0.825	261.75	258.09	1.40	0.6891	0.6883	0.12
*r*1	3.1264	0.1319	0.4380	0.4016	−0.438	0.584	0.9855	0.861	221.38	219.04	1.06	0.7109	0.7105	0.06
*r*2	3.2198	0.1281	0.4615	0.4022	−0.292	0.584	0.9856	0.898	186.18	181.93	2.28	0.7314	0.7322	0.11
*r*3	3.3190	0.1243	0.4749	0.4028	−0.146	0.584	0.9857	0.935	144.02	146.75	1.90	0.7516	0.7536	0.27
*r*4	3.4100	0.1210	0.4796	0.4034	0.000	0.584	0.9859	0.971	106.11	113.52	6.98	0.7740	0.7747	0.08
*r*5	3.5063	0.1176	0.4761	0.4040	0.146	0.584	0.9862	1.007	81.42	82.23	1.00	0.7948	0.7953	0.06
*r*6	3.5988	0.1146	0.4638	0.4044	0.292	0.584	0.9864	1.044	45.90	52.88	15.21	0.8150	0.8156	0.07
*r*7	3.6841	0.1120	0.4412	0.4048	0.438	0.584	0.9867	1.081	20.59	25.47	23.70	0.8364	0.8355	0.11
*r*8	3.7705	0.1094	0.4052	0.4052	0.584	0.584	0.9872	1.117	0.00	0.00	0.00	0.8550	0.855	0.00
*ra*0	2.9654	0.1391	0.4585	0.4584	−0.300	0.300	0.9845	0.8250	131.34	132.58	0.95	0.6894	0.6883	0.16
*ra*1	3.0046	0.1373	0.4645	0.4587	−0.250	0.300	0.9846	0.8376	118.10	120.28	1.85	0.6971	0.6959	0.17
*ra*2	3.0438	0.1355	0.4692	0.4591	−0.200	0.300	0.9847	0.8499	106.33	108.21	1.77	0.7047	0.7035	0.17
*ra*3	3.0816	0.1339	0.4730	0.4594	−0.150	0.300	0.9848	0.8628	94.98	96.36	1.46	0.7120	0.7111	0.13
*ra*4	3.1215	0.1321	0.4757	0.4597	−0.100	0.300	0.9849	0.8747	84.74	84.75	0.01	0.7192	0.7185	0.09
*ra*6	3.1988	0.1290	0.4782	0.4602	0.000	0.300	0.9850	0.9003	63.43	62.19	1.95	0.7331	0.7334	0.04
*ra*8	3.2705	0.1261	0.4768	0.4608	0.100	0.300	0.9852	0.9248	41.29	40.55	1.79	0.7471	0.7481	0.13
*ra*10	3.3434	0.1234	0.4714	0.4612	0.200	0.300	0.9853	0.9502	19.11	19.82	3.72	0.7618	0.7626	0.11
*ra*12	3.4120	0.1209	0.4617	0.4617	0.300	0.300	0.9855	0.9750	0.00	0.00	0.00	0.7772	0.7769	0.03
*s*0	2.9447	0.1401	0.4761	0.4761	0.000	0.000	0.9844	0.8251	0.00	0.00	0.00	0.6892	0.6883	0.13
*s*1	3.1106	0.1326	0.4756	0.4756	0.100	0.100	0.9848	0.8749	0.00	0.00	0.00	0.7192	0.7185	0.09
*s*2	3.2718	0.1261	0.4709	0.4709	0.200	0.200	0.9851	0.9251	0.00	0.00	0.00	0.7471	0.7481	0.13
*s*3	3.4098	0.1210	0.4617	0.4617	0.300	0.300	0.9855	0.9751	0.00	0.00	0.00	0.7772	0.7769	0.03
*s*4	3.5521	0.1161	0.4476	0.4476	0.400	0.400	0.9859	1.0250	0.00	0.00	0.00	0.8077	0.8051	0.33
*s*5	3.6721	0.1123	0.4276	0.4276	0.500	0.500	0.9865	1.0748	0.00	0.00	0.00	0.8340	0.8325	0.18
*s*6	3.7896	0.1088	0.4002	0.4002	0.600	0.600	0.9874	1.1246	0.00	0.00	0.00	0.8583	0.8592	0.11
*t*0	4.1910	0.1074	0.4066	0.4064	−0.584	0.584	0.9889	0.9002	259.49	258.09	0.54	0.6868	0.6883	0.22
*t*1	4.0812	0.1103	0.4062	0.4426	−0.584	0.438	0.9884	0.8638	238.37	232.62	2.41	0.6640	0.6658	0.27
*t*2	3.9767	0.1131	0.4057	0.4652	−0.584	0.292	0.9881	0.8265	200.25	205.21	2.48	0.6400	0.6429	0.45
*t*3	3.8632	0.1165	0.4053	0.4775	−0.584	0.146	0.9879	0.7906	174.58	175.86	0.73	0.6180	0.6196	0.26
*t*4	3.7387	0.1204	0.4047	0.4810	−0.584	0.000	0.9878	0.7543	142.62	144.57	1.37	0.5965	0.5959	0.09
*t*5	3.6102	0.1246	0.4041	0.4761	−0.584	−0.146	0.9876	0.7172	106.36	111.34	4.68	0.5738	0.5719	0.33
*t*6	3.4765	0.1294	0.4033	0.4625	−0.584	−0.292	0.9874	0.6807	71.35	76.17	6.75	0.5493	0.5475	0.32
*t*7	3.3391	0.1348	0.4025	0.4387	−0.584	−0.438	0.9873	0.6447	35.36	39.05	10.45	0.5233	0.5227	0.11
*t*8	3.1712	0.1419	0.4015	0.4015	−0.584	−0.584	0.9875	0.6080	0.00	0.00	0.00	0.4955	0.4976	0.42
*u*1	2.9500	0.1398	0.4683	0.4685	−0.200	0.200	0.9845	0.8248	87.34	88.39	1.20	0.6893	0.6883	0.15
*u*2	2.9800	0.1384	0.4436	0.4438	−0.400	0.400	0.9846	0.8249	175.39	176.78	0.79	0.6895	0.6883	0.17
*u*3	3.0500	0.1355	0.3951	0.3953	−0.600	0.600	0.9847	0.8266	266.39	265.16	0.46	0.6884	0.6883	0.01
*u*4	3.1500	0.1310	0.2968	0.2970	−0.800	0.800	0.9850	0.8253	356.87	353.55	0.93	0.6884	0.6883	0.01

NOTE.—Cols. (2)–(9) give the puncture initial location $\pm x/M$, the linear momenta $\pm p/M$, the mass parameters m_i/M, the dimensionless spins a_i, the normalized ADM mass $\tilde{M}_{\rm ADM} \equiv M_{\rm ADM}/M$ measured at infinity, and the normalized ADM angular momentum $\tilde{J}_{\rm ADM} \equiv J_{\rm ADM}/M^2$. Cols. (10)–(15) contain the numerical and fitted values for $|v_{\rm kick}|$ (in km s^{-1}), $a_{\rm fin}$, and the corresponding errors.

method, which allows one to choose the initial data parameters such that the resulting physical parameters (e.g., masses and spins) describe a binary black hole system on a quasi-circular orbit. The free parameters are: the coordinate locations $\mathbf{C}_i$, the mass parameters m_i, the linear momenta $\mathbf{p}_i$, and the spins $\mathbf{S}_i$. Quasi-circular orbits are then selected by setting $\mathbf{p}_1 = -\mathbf{p}_2$ to be orthogonal to $\mathbf{C}_2 - \mathbf{C}_1$, so that $\mathbf{L} \equiv \mathbf{C}_1 \times \mathbf{p}_1 + \mathbf{C}_2 \times \mathbf{p}_2$ is the orbital angular momentum. The initial parameters are collected in the left part of Table 1, while the right part reports the results of simulations. For all of them we have employed 8 levels of refinement and a minimum resolution $0.024M$, which has been reduced to $0.018M$ for binaries *r*5 and *r*6. Note that our results for the *u*-sequence differ slightly from those reported by Herrmann et al. (2007b), probably because of our accounting of the integration constant in $|v_{\rm kick}|$ (Pollney et al. 2007).

3. SPIN DIAGRAMS AND FITS

Clearly, the recoil velocity and the spin of the final black hole are among the most important pieces of information to be extracted from the inspiral and coalescence of binary black holes. For binaries with equal masses and aligned but otherwise arbitrary spins, this information depends uniquely on the dimensionless spins of the two black holes a_1 and a_2, and can therefore be summarized in the portion of the (a_1, a_2) plane in which the two spins vary. It is therefore convenient to think in terms of "spin diagrams," which summarize in a simple way all of the relevant information. In addition, since the labeling "1" and "2" is arbitrary, the line $a_1 = a_2$ in the spin diagram has important symmetries: the recoil velocity vector undergoes a π-rotation, i.e., $\boldsymbol{v}_{\rm kick}(a_1, a_2) = -\boldsymbol{v}_{\rm kick}(a_2, a_1)$, but $|v_{\rm kick}(a_1, a_2)| = |v_{\rm kick}(a_2, a_1)|$,

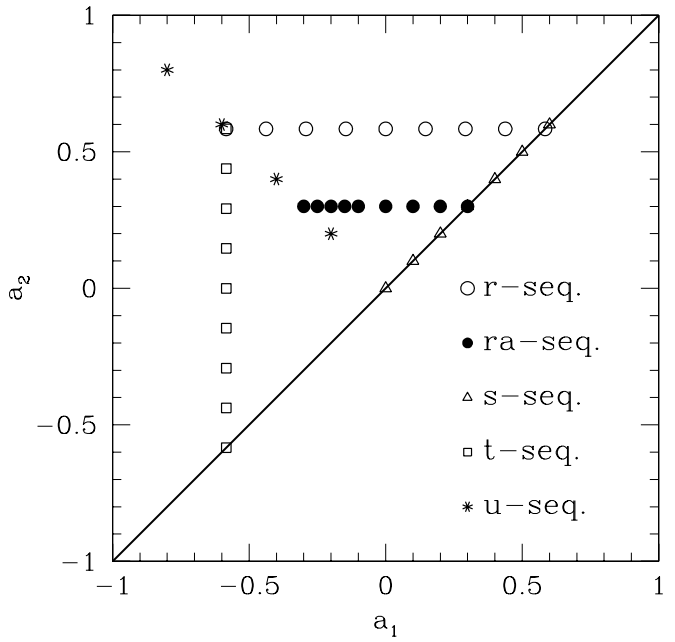

FIG. 1.—Position in the (a_1, a_2) space of the five sequences *r*, *ra*, *s*, *t*, and *u* for which the inspiral and merger has been computed. [*See the electronic edition of the Journal for a color version of this figure.*]

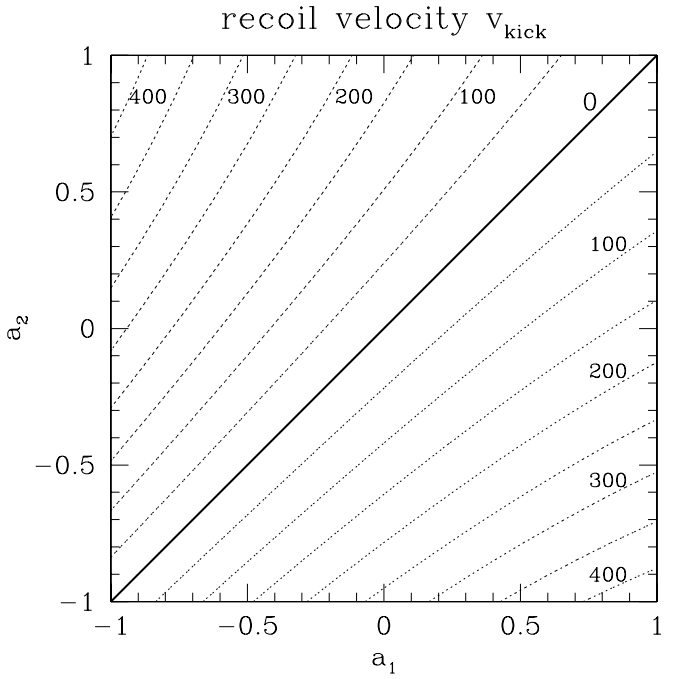

FIG. 2.—Contour plots of $|v_{\rm kick}|$ as a function of the spin parameters a_1 and a_2. The diagram has been computed using eqs. (4) and (5). [*See the electronic edition of the Journal for a color version of this figure.*]

while no change is expected for the final spin, i.e., $a_{\rm fin}(a_1, a_2) = a_{\rm fin}(a_2, a_1)$. These symmetries not only allow us to consider only one portion of the (a_1, a_2) space (cf. Fig. 1), thus halving the computational costs (or doubling the statistical sample), but they will also be exploited later on to improve our fits. The position of the five sequences within the (a_1, a_2) space is shown in Figure 1.

Overall, the data sample computed numerically consists of 38 values for $|v_{\rm kick}|$ and for $a_{\rm fin}$, which, for simplicity, we have considered to have constant error bars of 8 km s^{-1} and 0.01, which represent the largest errors reported in Pollney et al. (2007). In both cases we have modeled the data with generic quadratic functions in a_1 and a_2 so that, in the case of the recoil velocity, the fitting function is

$$|v_{\rm kick}| = \left|c_0 + c_1 a_1 + c_2 a_1^2 + d_0 a_1 a_2 + d_1 a_2 + d_2 a_2^2\right|. \quad (1)$$

Note that the fitting function on the right-hand side of equation (1) is smooth everywhere but that its absolute value is not smooth along the diagonal $a_1 = a_2$. Using equation (1) and a blind least-square fit of the data, we obtained the coefficients (in km s^{-1})

$$\begin{aligned} c_0 &= 0.67 \pm 1.12, \quad & d_0 &= -18.56 \pm 5.34, \\ c_1 &= -212.85 \pm 2.96, \quad & d_1 &= 213.69 \pm 3.57, \\ c_2 &= 50.85 \pm 3.48, \quad & d_2 &= -40.99 \pm 4.25, \end{aligned} \quad (2)$$

with a reduced $\chi^2 = 0.09$. Clearly, the errors in the coefficients can be extremely large; this is simply the result of small-number statistics. However, the fit can be improved by exploiting some knowledge of the physics of the process to simplify the fitting expressions. In particular, we can use the constraint that no recoil velocity should be produced for binaries having the same spin, i.e., that $|v_{\rm kick}| = 0$ for $a_1 = a_2$, or the symmetry condition across the line $a_1 = a_2$. Enforcing both constraints yields

$$c_0 = 0, \quad c_1 = -d_1, \quad c_2 = -d_2, \quad d_0 = 0, \quad (3)$$

thus reducing the fitting function of equation (1) to the simpler expression

$$|v_{\rm kick}| = \left|c_1(a_1 - a_2) + c_2(a_1^2 - a_2^2)\right|. \quad (4)$$

Performing a least-square fit using equation (4), we then obtain

$$c_1 = -220.97 \pm 0.78, \quad c_2 = 45.52 \pm 2.99, \quad (5)$$

with a comparable reduced $\chi^2 = 0.14$, but with error bars that are much smaller on average. Because of this, we consider equation (4) as the best description of the data at second-order in the spin parameters. Using equations (4) and (5), we have built the contour plots shown in Figure 2.

A few remarks are worth making. First, we recall that post-Newtonian calculations have so far derived only the linear contribution in the spin to the recoil velocity (see Favata et al. 2004, and references therein). However, the size of the quadratic coefficient (eq. [5]) is not small when compared to the linear one, and it can lead to rather sizeable corrections. These are maximized when $a_1 = 0$ and $a_2 = \pm 1$, or when $a_1 = \pm 1$ and $a_2 = 0$, and can be as large as $\sim$20%; while these corrections are smaller than those induced by asymmetries in the mass, they are instructive in pointing out the relative importance of spin-spin and spin-orbit effects during the merger, and can be used as a guide in further refinements of the post-Newtonian treatments. Second, equation (4) clearly suggests that the maximum recoil velocity should be found when the asymmetry is largest and the spins are antiparallel, i.e., $a_1 = -a_2$. Third, when $a_2 = $ const., equation (4) confirms the quadratic scaling proposed in Pollney et al. (2007) with a smaller data set (cf. their eq. [42]). Fourth, for $a_1 = -a_2$, equation (4) is only linear and reproduces the scaling suggested by Herrmann et al. (2007b). Finally, using equation (4) the maximum recoil velocity is found to be $|v_{\rm kick}| = 441.94 \pm 1.56$ km s^{-1}, in very good agreement with the results of Herrmann et al. (2007b) and Pollney et al. (2007).

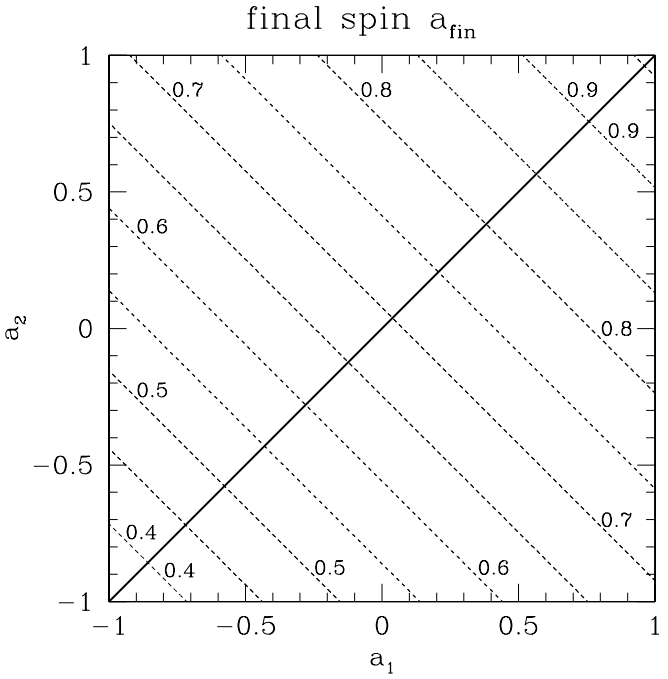

FIG. 3.—Contour plots of $a_{\rm fin}$ as a function of the spin parameters a_1 and a_2. The diagram has been computed using eqs. (8) and (9). [*See the electronic edition of the Journal for a color version of this figure.*]

In the same way, we have first fitted the data for $a_{\rm fin}$, with a function

$$a_{\rm fin} = p_0 + p_1 a_1 + p_2 a_1^2 + q_0 a_1 a_2 + q_1 a_2 + q_2 a_2^2, \quad (6)$$

and found coefficients with very large error bars. As a result, for $a_{\rm fin}$ as well we resort to physical considerations to constrain the coefficients $p_0 \ldots q_2$. More specifically, we expect that, at least at lowest order, binaries with equal and opposite spins will not contribute to the final spin, and thus behave essentially as nonspinning binaries. Stated differently, we assume that $a_{\rm fin} = p_0$ for binaries with $a_1 = -a_2$. In addition, enforcing the symmetry condition across the line $a_1 = a_2$, we obtain

$$p_1 = q_1, \quad p_2 = q_2 = q_0/2, \quad (7)$$

so that the fitting function given by equation (6) effectively reduces to

$$a_{\rm fin} = p_0 + p_1(a_1 + a_2) + p_2(a_1 + a_2)^2. \quad (8)$$

Performing a least-square fit using equation (8), we then obtain

$$p_0 = 0.6883 \pm 0.0003, \quad p_1 = 0.1530 \pm 0.0004, \quad p_2 = -0.0088 \pm 0.0005, \quad (9)$$

with a reduced $\chi^2 = 0.02$.

It should be noted that the coefficient of the quadratic term in equation (9) is much smaller then the linear one and with much larger error bars. Given the small statistics, it is hard to assess whether a quadratic dependence is necessary or if a linear one is correct (however, see also the comment below on a possible interpretation of eq. [8]). In view of this, we have repeated the least-square fit of the data enforcing the conditions of equation (7) together with $p_2 = 0$ (i.e., adopting a linear fitting function) and obtained $p_0 = 0.6855 \pm 0.0007$ and $p_1 = 0.1518 \pm 0.0012$, with a worse reduced $\chi^2 = 0.16$. Because the coefficients of the lowest order terms are so similar, both the linear and the quadratic fits are well within the error bars of the numerical simulations. Nevertheless, since a quadratic scaling yields smaller residuals, we consider it to be the best representation of the data and have therefore computed the contour plots in Figure 3 using equations (8) and (9).

Here too, a few remarks are worth making. First, the fitted value for the coefficient p_0 agrees very well with the values reported by several groups (Gonzalez et al. 2007b; Berti et al. 2007) when studying the inspiral of unequal-mass nonspinning binaries. Second, equation (8) has maximum values for $a_1 = a_2$, suggesting that the maximum and minimum spins are $a_{\rm fin} = 0.9591 \pm 0.0022$ and $a_{\rm fin} = 0.3471 \pm 0.0224$, respectively. Third, the quadratic scaling for $a_{\rm fin}$ substantially confirms the suggestions of Campanelli et al. (2006b), but provides more accurate coefficients. Finally, although very simple, equation (9) lends itself to an interesting interpretation. Being effectively a power series in terms of the initial spins of the two black holes, its zeroth-order term can be seen as the orbital angular momentum not radiated in gravitational waves and which amounts, at most, to $\sim$70% of the final spin. The first-order term, on the other hand, can be seen as the contribution to the final spin coming from the initial spins of the two black holes, and this contribution, together with the one coming from the spin-orbit coupling, amounts at most to $\sim$30% of the final spin. Then the second-order term, which is natural to expect as nonzero in this view, can be related to the spin-spin coupling, with a contribution to the final spin that is $\sim$4% at most.

As a side remark, we also note that the monotonic behavior expressed by equation (9) does not show the presence of a local maximum of $a_{\rm fin} \simeq 0.87$ for $a_1 = a_2 \sim 0.34$ as suggested by Damour (2001) in the effective one-body (EOB) approximation. Because the latter has been shown to be in good agreement with numerical-relativity simulations of nonspinning black holes (Damour & Nagar 2007; Damour et al. 2007), additional simulations will be necessary to refute these results or to improve the EOB approximation for spinning black holes.

Reported in the right part of Table 1 are also the fitted values for $a_{\rm fin}$ and $|v_{\rm kick}|$ obtained through the fitting functions (4) and (8), and the corresponding errors. The latter are of few percent for most cases and increase up to $\sim$20% only for those binaries with very small kicks and which are intrinsically more difficult to calculate. As a concluding remark, we note that the fitting coefficients computed here have been constructed using overall moderate values of the initial spin; the only exception is the binary $u4$, which has the largest spin and which is nevertheless fitted with very small errors (cf. Table 1). In addition, since the submission of this work, another group has reported results from equal-mass binaries with spins as high as $a_1 = a_2 = \pm 0.9$ (Marronetti et al. 2008). Although for these very high-spin binaries the error in the predicted values is also of 1% at most, a larger sample of high-spin binaries is necessary to validate that the fitting expressions (4) and (8) are robust also at very large spins.

4. CONCLUSIONS

We have performed least-square fits to a large set of numerical-relativity data. These fits, combined with symmetry arguments, yield analytic expressions for the recoil velocity and final black hole spin resulting from the inspiral and merger of equal-mass black holes whose spins are parallel or antiparallel to the orbital angular momentum. Such configurations represent a small portion of the parameter space, but may be the preferred ones if

torques are present during the evolution. Using the analytic expressions we have constructed two spin diagrams that summarize this information simply and predict a maximum recoil velocity of $|v_{\rm kick}| = 441.94 \pm 1.56\,{\rm km\,s^{-1}}$ for systems with $a_1 = -a_2 = 1$ and maximum (minimum) final spin $a_{\rm fin} = 0.9591 \pm 0.0022$ (0.3471 ± 0.0224) for systems with $a_1 = a_2 = 1$ (-1).

Note added in manuscript.—Since the publication of this analysis on the preprint archive, our work on the modelling of the final spin has progressed rapidly, yielding new results that complement and complete the ones presented here. In particular, the work published in Rezzolla et al. (2008b) complements the analysis carried here to unequal-mass, equal-spin aligned binaries, while the work reported in Rezzolla et al. (2008a) extends it to generic binaries.

It is a pleasure to thank Thibault Damour and Alessandro Nagar for interesting discussions. The computations were performed on the supercomputing clusters of the AEI. This work was supported in part by the DFG grant SFB/Transregio 7.

REFERENCES

Baker, J. G., Centrella, J., Choi, D.-I., Koppitz, M., & van Meter, J. 2006a, Phys. Rev. D, 73, 104002
Baker, J. G., Centrella, J., Choi, D.-I., Koppitz, M., van Meter, J. R., & Miller, M. C. 2006b, ApJ, 653, L93
Berti, E., Cardoso, V., Gonzalez, J. A., Sperhake, U., Hannam, M., Husa, S., & Bruegmann, B. 2007, Phys. Rev. D, 76, 064034
Bogdanovic, T., Reynolds, C. S., & Miller, M. C. 2007, ApJ, 661, L147
Bonning, E. W., Shields, G. A., Salviander, S. 2007, ApJ, 666, L13
Campanelli, M., Lousto, C. O., Marronetti, P., & Zlochower, Y. 2006a, Phys. Rev. Lett., 96, 111101
Campanelli, M., Lousto, C. O., & Zlochower, Y. 2006b, Phys. Rev. D, 73, 061501(R)
Campanelli, M., Lousto, C. O., Zlochower, Y., & Merritt, D. 2007a, ApJ, 659, L5
———. 2007b, Phys. Rev. Lett., 98, 231102
Damour, T. 2001, Phys. Rev. D, 64, 124013
Damour, T., & Nagar, A. 2007, Phys. Rev. D, 76, 044003
Damour, T., Nagar, A., Dorband, E. N., Pollney, D., & Rezzolla, L. 2007, Phys. Rev. D, 76, 064028
Favata, M., Hughes, S. A., Holz, D. E. 2004, ApJ, 607, L5
Gonzalez, J. A., Hannam, M. D., Sperhake, U., Brugmann, B., & Husa, S. 2007a, Phys. Rev. Lett., 98, 231101
Gonzalez, J. A., Sperhake, U., Bruegmann, B., Hannam, M., & Husa, S. 2007b, Phys. Rev. Lett., 98, 091101
Herrmann, F., Hinder, I., Shoemaker, D., & Laguna, P. 2007a, Classical Quantum Gravity, 24, S33
Herrmann, F., Hinder, I., Shoemaker, D., Laguna, P., & Matzner, R. A. 2007b, Phys. Rev. D, 76, 084032
Koppitz, M., Pollney, D., Reisswig, C., Rezzolla, L., Thornburg, J., Diener, P., & Schnetter, E. 2007, Phys. Rev. Lett., 99, 041102
Loeb, A. 2007, Phys. Rev. Lett., 99, 041103
Marronetti, P. Tichy, W., Brügmann, B., González, J., & Sperhake, U. 2008, Phys. Rev. D, 77, 064010
Pollney, D., et al. 2007, Phys. Rev. D, 76, 124002
Rezzolla, L., Barausse, E., Dorband, E. N., Pollney, D., Reisswig, C., & Seiler, J. 2008a, preprint (arXiv:0712.3541)
Rezzolla, L., Diener, P., Dorband, E. N., Pollney, D., Reisswig, C., Schnetter, E., & Seiler, J. 2008b, ApJ, 674, L29
Schnetter, E., Hawke, I., & Hawley, S. H. 2004, Classical Quantum Gravity, 21, 1465
Schnittman, J. D. 2004, Phys. Rev. D, 70, 124020